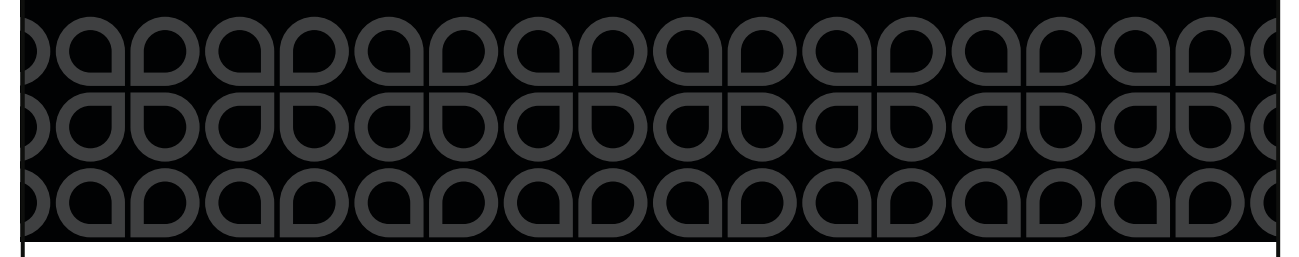
Chemistry A European Journal





Accepted Article

Title: Syntheses of Carbazoles by Photosensitized Electrocyclization of Triarylamines. Effect of Inductive Electron-Withdrawing Groups on the Photocyclization.

Authors: Ivan E. Romero, Margarita M. Vallejos, Sebastian Barata-Vallejo, Sergio M. Bonesi, and Al Postigo

This manuscript has been accepted after peer review and appears as an Accepted Article online prior to editing, proofing, and formal publication of the final Version of Record (VoR). The VoR will be published online in Early View as soon as possible and may be different to this Accepted Article as a result of editing. Readers should obtain the VoR from the journal website shown below when it is published to ensure accuracy of information. The authors are responsible for the content of this Accepted Article.

To be cited as: Chem. Eur. J. 2025, e202500133

Link to VoR: https://doi.org/10.1002/chem.202500133

RESEARCH ARTICLE

Syntheses of Carbazoles by Photosensitized Electrocyclization of Triarylamines. Effect of Inductive Electron-Withdrawing Groups on the Photocyclization.

Ivan E. Romero,^[a,b] Margarita M. Vallejos,^[c] Sebastian Barata-Vallejo,^[a,d] Sergio M. Bonesi,*^[b] Al Postigo*^[a]

[a] Ivan E. Romero, Prof. Dr. Sebastian Barata-Vallejo, Prof. Dr. Al Postigo*

Departamento de Ciencias Químicas.

Facultad de Farmacia y Bioquímica, Universidad de Buenos Aires.

Junin 954-CP 1113-Buenos Aires-Argentina

E-mail: apostigo@ffyb.uba

[b] Ivan E. Romero, Prof. Dr. S. M. Bonesi*.

Departamento de Química Orgánica.

Facultad de Ciencias Exactas y Naturales, Universidad de Buenos Aires. Ciudad Universitaria, Buenos Aires C1428EGA-Argentina and CONICET-

Universidad de Buenos Aires. Centro de Investigaciones en Hidratos de Carbono. (CIHIDECAR). Argentina.

Ciudad Universitaria. Buenos Aires. C1428EGA.

Email: smbonesi@qo.fcen.uba.ar

[c] Dr. Margarita M. Vallejos.

Departamento de Química, IQUIBA-NEA.

Universidad Nacional del Nordeste, CONICET, FACENA.

Av. Libertad 5460, Corrientes 3400, Argentina.

[d] Prof. Dr. Sebastian Barata-Vallejo.

Istituto per la Sintesi Organica e la Fotoreattività ISOF Consiglio Nazionale delle Ricerche.

Via P. Gobetti 101, 40129, Bologna (Italy).

Supporting information for this article is given via a link at the end of the document.

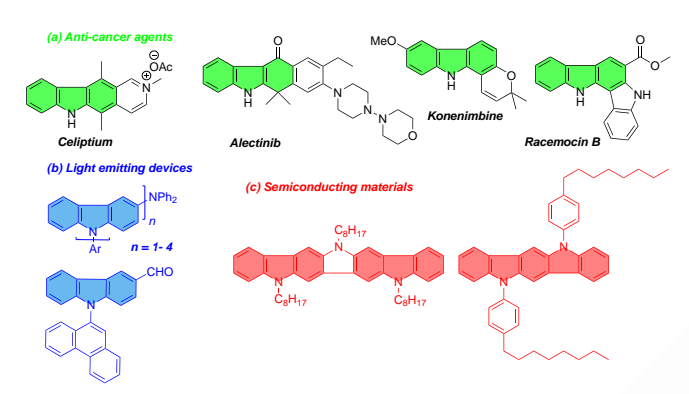
The acetone-sensitized [6π]-electrocyclization of unsubstituted, mono-, and disubstituted triarylamines (TAAs: substituents H, CH₃, CH₃O, CI, C_nF_{2n+1} ; n = 1, 3, 4, 6, 8, 10) under 310 nm light led to the formation of endo- and exo-carbazoles in high yields; particularly, TAAs substituted with inductive electronwithdrawing groups (Cl, C_nF_{2n+1}) exhibit remarkable endo-selectivity towards cyclization. For TAAs substituted with both inductive electronwithdrawing and donating groups, the photocyclization towards endo carbazoles is dictated by the presence of the electron-withdrawing groups. Chemical yields (%), quantum yields of conversion (ϕ_R), apparent cyclization rate constants (k_{cyc}), and Hammett plots correlations are illustrated for all substituted TAAs in acetone. Photophysical studies reveal that TAAs substituted with resonance electron-withdrawing groups (OAc, NO2, CHO) do not undergo electrocyclization in acetone at 310 nm due to formation of chargetransfer states that vastly deactivate the triplet reactive manifold, paralleling the behavior observed in MeCN as solvent. Absorption and emission spectra, Stokes shifts, and singlet excited state energies are illustrated for substituted TAAs and carbazoles. In-silico studies support the high stereoselectivity observed for the preferred endophotosensitized [6\pi]-electrocyclization of Cl- and perfluoroalkylsubstituted TAAs

Introduction

Carbazole, a typical nitrogen-containing heterocycle, can be considered as an interesting and "privileged" motif in organic chemistry. This heterocycle scaffold can be found in natural products, bioactive molecules, pharmaceuticals, and materials science.[1] Indeed, ellipticine derivatives, Stauroporine, Carbazomycin B, Carazolol, and Carvedilol are pharmacophores showing the carbazole moiety in their structures^[2] and some of these bioactive carbazoles are useful in the treatment of ischemic hypertension, and congestive heart Furthermore, carbazole and its derivatives were found to show optoelectronic,[4] electronic and structural features as lightemitting,[5] polymer,[6] conducting and charge transporting/host materials.[7] Some selected examples are depicted in Scheme 1.

Incorporation of trifluoromethyl and perfluoroalkyl groups in (hetero)arenes, and particularly in carbazoles, has a notable impact on the physical and biological properties of these compounds, providing metabolic stability and lipophilicity due to the electron-withdrawing nature of the perfluoroalkyl substituent. [8] Polymers bearing perfluoroalkyl groups provide hydrophobic and oleophobic behaviors. [9] Therefore, based on the properties displayed by carbazoles as highly relevant scaffolds, diverse synthetic methodologies have been developed. [10] Recently, an interesting review has updated a variety of preparative methodologies of carbazoles involving thermal, photochemical and electrochemical approaches. [11]

Different synthetic routes toward the preparation of carbazole moieties including nitrene insertion, Fischer indolization, dehydrogenative cyclization of diarylamines, Pummerer cyclization, and Diels-Alder reaction, among others, have been reported. [12] Furthermore, C-C and C-N bond formations involving transition-metal catalysts were found to be useful in the preparation of carbazoles. [13,14] In fact, Pd-catalyzed C-C bond formation and Pt-catalyzed C-H activation have been carried out successfully providing the desired carbazoles. [15] However, these thermal methodologies are performed under high reaction temperature, long reaction times and employing expensive transition metal catalysts and phosphorous ligands.



Scheme 1. Structural examples of anti-cancer agents, emitting and semiconducting materials containing the carbazole moiety

On the other hand, direct perfluoroalkylation of carbazole moiety remains almost unexplored whereas perfluoroalkylated carbazoles have been prepared involving coupling reactions of carbazoles with perfluoroalkylated aryl rings. [16] In fact, the late-stage perfluoroalkylation of carbazoles has been achieved successfully involving UV irradiation of an excess of C₄F₉I in aqueous media. [17] Likewise, visible light irradiation of 2,3-dichloro-5,6-dicyano-*p*-benzoquinone in the presence of Langlois reagent led to the formation of trifluoromethylcarbazole but with low yield and very poor regioselectivity. [18]

The photochemical methodology is an interesting, mild, and alternative procedure to be applied for the preparation of carbazoles. Indeed, photocatalytic oxidative C-C bond coupling of di- and triarylamines and aryl azides has been carried out under flow conditions employing visible light and transition-metal complexes as the photocatalysts as well as direct irradiation with UV light in the presence of propylene oxide and iodine.[19] However, expensive photocatalysts, use of specific ligands and the requirement of continuous flow setups make this methodology a limited procedure to perform the photoreaction. Furthermore, long reaction times are needed and, if the irradiations are conducted under batch conditions, conversion to products may take several weeks. Iridium photocatalyst combined with catalytic amounts of Pd(OAc)₂ led to the preparation of a set of carbazoles including the synthesis of alkaloid Clausine C from oaminobiphenyls through a C-N oxidative coupling.[20] Photosensitized Cadogan-type reaction through triplet energy transfer process of o-nitrobiaryls has recently been reported using 4CzIPN and Ir[dF(CF₃)ppy]₂(dtbpy)PF₆ as the photosensitizers.^[21] Direct irradiation of di- and triarylamine with UV light is a photochemical procedure that leads to substituted carbazoles in quantitative yields under molecular oxygen as the sole oxidant reagent since its discovery in the 1960s when carbazole was prepared from diphenylamine. [22,23] This UV light driven oxidative $[6\pi]$ -electrocyclization reaction was also extended to Nmethyldiphenylamine^[24] and triphenylamine.^[25] Furthermore, quenching of the triplet-triplet energy transfer process with triplet acceptors as well as triplet sensitization by aromatic ketones of the photocyclization reaction of diphenylamines have amply demonstrated that the photo reactive excited state is the lowest triplet state. [23a,24a,24b,24d,25a] Steady-state and time-resolved investigations on the photoinduced $[6\pi]$ -electrocyclization reaction of di-and triarylamines have been reported. [26] Indeed, cooxidation of alkyl/aryl sulfides and triarylphosphines proceeded successfully with triarylamines as the oxidizing photosensitizers in the presence of molecular oxygen. [25c,26a,b]

The solvent effect on the photocyclization reaction of di- and triphenylamines has also been carried out in homogeneous and micro heterogeneous media where carbazoles were obtained in quantitative yields. [26c-e] Micellar media showed that the [6 π]electrocyclization reaction was accelerated when compared with homogeneous media. The substituent effect on the photocyclization reaction of mono-, di- and trisubstituted triphenylamine has recently been reported and electron-donor and neutral substituents promoted the photoreaction efficiently forming exo/endo carbazoles in modest to good yields.[27a] Likewise, the solvent effect on the photoreaction was also investigated and the exo/endo carbazoles formation was favored in polar solvents over nonpolar ones.[27b] However, the photoreaction of triphenylamine bearing electron-withdrawing (resonance) substituents did not proceed due to the formation of intramolecular charge transfer states. It is worthy to mention that, for TPAs substituted with electron-donating and neutral substituents, all these photocyclizations were carried out successfully under mild conditions and in the presence of molecular oxygen.

Recently, a photochemical perfluoroalkylation reaction of triphenylamine has been developed leading to the efficient preparation of monoperfluoroalkylated triphenylamines in good yields. [28] Direct irradiation with blue LEDs of an Electron Donor Acceptor (EDA) complex formed between N,N,N',N'tetramethylethylenediamine (TMEDA) and perfluoroalkyl iodides (R_FI) in the presence of triphenylamine in aqueous solvent mixture afforded the expected mono perfluoroalkyltriphenylamines. According to our knowledge, this interesting and efficient methodology is currently the first established late-stage protocol available for the synthesis of perfluoroalkyl-substituted triphenylamines. In fact, the preexisting synthetic methods for the preparation of trifluoromethyl triphenylamines primarily rely on indirect protocols rather than direct synthetic approaches.[29] Regarding the realm of perfluoroalkylation reactions, several contributions from our research group developing perfluoroalkyl radicals through visible-light photocatalysis have been reported leading to the incorporation of perfluoroalkyl groups into diverse organic frameworks.[30]

RESEARCH ARTICLE

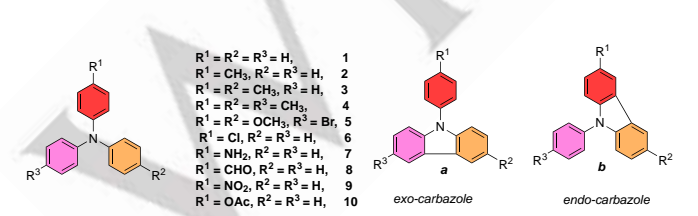
Based on these premises and knowing that the photoinduced $[6\pi]$ -electrocyclization reactions proceed from the triplet excited state of substituted triarylamines, we herein present a systematic study on the photosensitization of the $[6\pi]$ -electrocyclization reaction of several mono- and disubstituted triarylamines in acetone with light of 310 nm in the presence of molecular oxygen as the oxidant reagent (see Scheme 2). This investigation deals with the substituent effect on the product distribution analyzing the regiochemistry (exo/endo products) and the chemoselectivity (endo over exo products), the quantum yields of conversion (ϕ_R), and the apparent cyclization rate constants (k_{cyc}). Furthermore, spectroscopic behavior in terms of UV-visible absorption and fluorescence emission spectroscopies as well as fluorescence quantum yield (ϕ_f) measurements of substituted triarylamines and carbazoles are discussed. Computational calculations are conducted to rationalize the product distribution by analyzing free energy profiles for the [6π]-electrocyclization pathway from the triplet states of triarylamines. These calculations include optimized geometries of the transition state structures, their energies, spin density, C-C bond formation distances, and energy values of the dihydrocarbazole intermediates.



Scheme 2. The acetone-photosensitized $[6\pi]$ -electrocyclization reaction of mono and disubstituted triarylamines studied in this paper. From monosubstituted TAA, the *exo*-carbazole isomer bears the substituent in the *N*-phenyl ring, whereas in the *endo* isomer the substituent is in the carbazole scaffold

Results and Discussion

Photosensitized irradiation of triphenylamines with electron-donating and electron-withdrawing groups in acetone



Scheme 3. Triarylamines substituted with electron-neutral and donating substituents and electron withdrawing (resonance) substituents. The *exo*-isomer bears the substituent in the *N*-phenyl ring, whereas in the *endo* isomer the substituent is in the carbazole scaffold.

Triarylamines **2-10** (Scheme 3) were synthesized by literature procedures, [27a] and subjected to $[6\pi]$ -electrocyclization reactions in acetone, irradiating at 310 nm and employing a reaction setup depicted in Figure S1 (see ESI).

The comparative $[6\pi]$ -electrocyclizations of triarylamines **1-10** (Scheme 3) towards the respective carbazoles have been investigated in the past under 254 nm-direct irradiation in acetonitrile as solvent, and their photophysical properties studied.[27] The corollary of the study revealed several salient features: the exo/endo carbazole derivatives were formed as the main photoproducts from modest to good yields for triphenylamines substituted with electron-donor and neutral substituents. The kinetic parameters of the electrocyclization reactions showed dependence on the nature of the substituents, and linear Hammett correlations showcased the substituent effect. On the other hand, the spectroscopic behavior of the electron-rich substituted triphenylamines suggested that the fluorescence emission spectra display mirror images of the lower energy absorption bands, while for those amines bearing resonance electron-acceptor groups the formation of charge-transfer states and their fluorescence emissions constitute the main deactivation pathway of the photoreaction. In TPAs substituted with electronwithdrawing groups, especially by resonance effect, the formation of charge transfer states deactivates the triplet excited state responsible for electrocyclization.[27]

In another recent report, the acetone-sensitized electrocyclization (310 nm) of triarylamines substituted with perfluoroalkyl groups to yield perfluoroalkylated carbazoles in good yields was proposed as a convenient electrocyclization synthetic strategy. [28a] Based on these findings, we embarked, in this section, on the acetone-sensitization study of triarylamines **1-10** and analyzed the efficiency of cyclization and *endo/exo* carbazole ratios resulting from the $[6\pi]$ -electrocyclizations of these amines.

Table 1 illustrates the yields of the *exo/endo* carbazole products, along with the quantum yields of cyclization relative to triphenylamine 1, and the rates of cyclization in acetone.

As observed from Table 1, yields of cyclization in acetone are modest-to-high for TPA and TPAs substituted with electron-donating and CI groups (2-6). For TPAs 8-10, substituted with strong resonance electron-withdrawing groups, no $[6\pi]$ -electrocyclization product could be observed.

A particular example is TPA **7**, substituted with an activating amino group in *para* position of one phenyl ring, which did not electrocyclize under photosensitization in acetone to the respective carbazole, as observed in previous studies carried out in MeCN as solvent. [27a,b] This behavior can be attributed to the known electron transfer processes which result in the quenching of the triplet state of ketones by amines. [27e]

For TPAs **2-6**, sensitized irradiation of 4-substituted triphenylamines at 310 nm in acetone solution under either air or O₂ atmosphere led to the formation of two carbazole derivatives, *viz.*, *N*-(4-substituted-phenyl)carbazoles **2a – 6a** (column 6, Table 1), i.e.: exo carbazoles, and 3-substituted-*N*-phenylcarbazoles **2b – 6b** (column 7, Table 1) (see Scheme 3 for structures), i.e.: endocarbazoles.

Moreover, the formation of unsymmetric endo carbazoles **2b – 6b** occurs smoothly, and this unique behavior can be attributed to the different orbital coefficient values between the substituted and unsubstituted phenyl rings, which influence the electrocyclization pathway. The nature of the substituent attached to the phenyl ring—whether it is an electron-donor or electron-acceptor group—

RESEARCH ARTICLE

is expected to significantly alter the orbital coefficient values of the phenyl ring compared to the unsubstituted ones. This distribution of photoproducts has also been observed when triarylamines were irradiated under photocatalytic continuous flow conditions. [19b,c] We investigated this behavior by computational methods (vide infra In Silico Studies).

For the electron-rich mono-substituted TPAs **2**, **5**, and **6**, the *endo* carbazole product isomers prevail over the *exo* products (entries 2, 5, and 6, Table 1). For disubstituted 4-methyl-*N*-phenyl-*N*-(*p*-tolyl)aniline **3**, the *exo* carbazole isomer predominates over the *endo*, probably due to steric congestion in the electrocyclization pathway (entry 3, Table 1).

Table 1. Photosensitized irradiation of triphenylamines TPA in acetone: Chemical Yield, Quantum Yield (ϕ_R) , and rate of consumption of triphenylamines (1-10) under air atmosphere

| R ¹ | acetone (0.001 mol/dm³), 50 mL 310 nm, O ₂ , under stirring, 7 h 24 °C | R ¹ | + R ¹ |
|----------------|--|----------------|------------------|
| R ³ | | R" a " R" | ., р |

| | | | | | exo-carbaz | uie | endo-carbazole | | |
|-----|------------------|----------------|----------------|--------------------------|--------------------------------|-------------------------|-------------------------|-------------------|--|
| TPA | Sı | ıbstituent | S | | ole yield endo ra | | ф к ^с | rate,⁴ µM | |
| | R ¹ | R ² | R ³ | Yield, ^a % | a (exo) , ^b % | b (en do), b % | | min ⁻¹ | |
| 1 | Н | Н | Н | 98 | | | 0.010 | 0.113 | |
| 2 | CH ₃ | Н | Н | 95 | 26 | 74 | 0.010 | 0.121 | |
| 3 | CH₃ | CH₃ | Н | 96 | 66 | 34 | 0.013 | 0.129 | |
| 4 | CH₃ | CH₃ | CH₃ | 84 | | | 0.016 | 0.121 | |
| 5 | OCH ₃ | OCH₃ | Br | 80 | 28 | 72 | 0.011 | 0.088 | |
| 6 | CI | Н | Н | 48 | 24 | 76 | 0.015 | 0.247 | |
| 7 | NH ₂ | Н | Н | 0 | | | <0.00 | <0.00 1 | |
| 8 | CHO | Н | Н | 0 | | | <0.00 | <0.00 | |
| 9 | NO ₂ | Н | Н | 0 | 1 | | <0.00 1 | <0.00 | |
| 10 | COMe | Н | Н | 0 | | | <0.00 1 | <0.00 1 | |

a.- Yield obtained by HPLC integration with internal standard. b.- Ratio of isomers obtained through HPLC integration. c.- Quantum yield obtained based on reference quantum yield of unsubstituted TPA, $\phi_f = 0.050$ in acetonitrile. [33] d.- Rate obtained from Figure 1

The progress of the photochemical reaction of amines **1–10** was monitored using chromatographic (HPLC) analyses (Figure S2, ESI) with a UV-visible detector. For triphenylamines **8–10**, it was evident that no carbazole formation was detected in acetone by HPLC analyses, which was expected given the low quantum yield of the reactions, remaining around 10⁻³ (column 8, Table 1).

Both chemical yields of carbazoles and *exo/endo* ratios for TPAs **2 – 6** (Table 1) are similar to those found under direct irradiation at 254 nm in acetonitrile, indicating that both acetonesensitization and direct 254 nm-irradiation reach the same reactive triplet manifold with similar efficiency.^[27a] As opposed to the MeCN study,^[27b,c] TPA **7** does not electrocyclize to carbazole, as an electron transfer reaction supersedes the sensitization process.^[27e]

The relative yield profiles obtained from the acetone-sensitized irradiation (310 nm) of TPA (1) in an O_2 -saturated solution are shown in Figure S2a (ESI). The relative absorbance profiles indicate that as substrate 1 is consumed (expressed as the ratio A/A₀ at 310 nm), *N*-phenylcarbazole (*N*-PhCBz) is formed as the only photoproduct. In Figure S2c, the consumption of TPA 2 is followed as absorbance profiles indicating that as substrate 2 is consumed (expressed as the ratio A/A₀ at 310 nm), carbazoles (2a + 2b) are formed as the only photoproducts.

The rates of cyclization (Table 1, column 6) were determined from Figure 1, where the observed rate constants (slopes) for acetone-sensitized irradiation of triphenylamines (1 – 10) with light of 310 nm are extracted from the slopes through linear regression analyses between $ln(A/A_o)$ and time. It is observed that rates of cyclization are high from TPAs 2 - 6 with respect to TPA itself, and no $[6\pi]$ -electrocyclization is observed for TPAs substituted with resonance electron withdrawing groups (i.e.: 8 - 10).

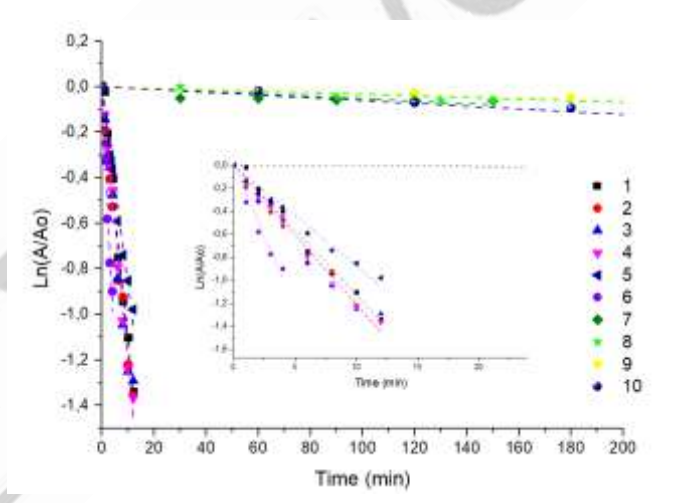
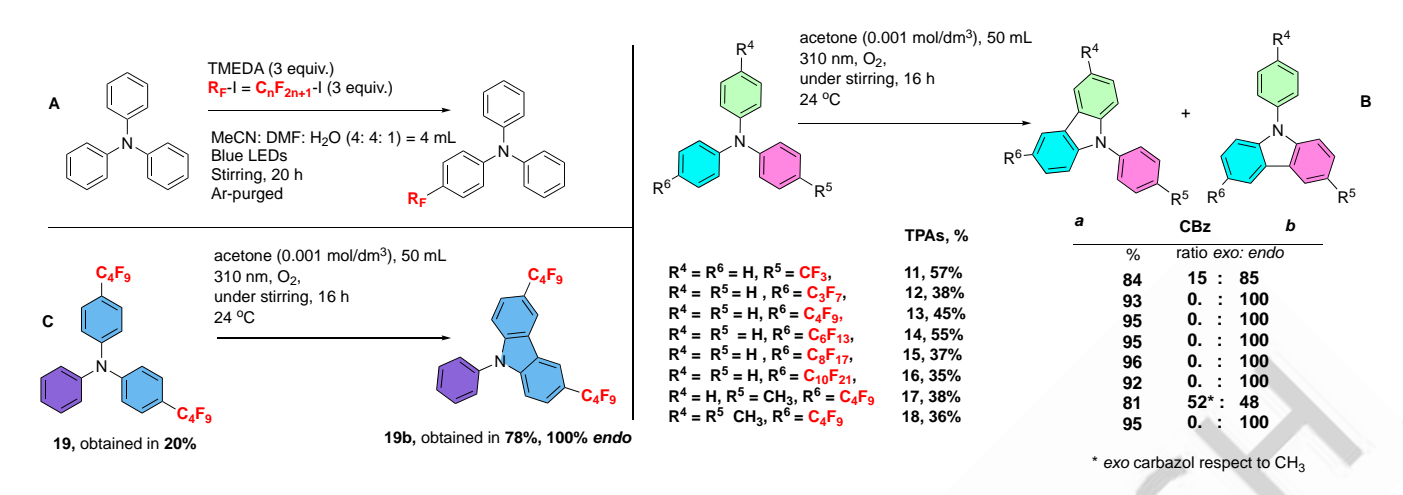


Figure 1. Longer time window (0 – 200 min) for the observed rate constants (k_{Obs}) for irradiated triphenylamines (1 – 10) in acetone with light of 310 nm. Linear regression between ln(A/Ao) and time. Inset: Shorter time window (0 – 24 min) for the observed rate constants (k_{Obs}) for irradiated triphenylamines (1 – 10) in acetone with light of 310 nm. Linear regression between ln(A/Ao) and time.

Photosensitized irradiation of triphenylamines substituted with inductively electron-withdrawing perfluoroalkyl groups

Triphenylamines **11-19** substituted with perfluoroalkyl groups R_F ($R_F = C_n F_{2n+1}$, n=1,3,4,6,8,10) were prepared by the procedure reported by us through irradiation of the electron donor acceptor (EDA) complexes between TMEDA and R_F -I in the presence of TPA in aqueous MeCN/ DMF solvent system. [28a] The general reaction is represented in Scheme 4A. The reaction setup is depicted in Figure S4 (see ESI). The resulting perfluoroalkylated triphenylamines were then subjected to the $[6\pi]$ -electrocyclization under acetone sensitization (310 nm) affording the corresponding substituted carbazoles (Schemes 4B, 4C).

RESEARCH ARTICLE



Scheme 4. A.- Syntheses of perfluoroalkyl-substituted triphenylamines 11-19. B.- Ulterior electrocyclization reaction of triphenylamines 11-18. C.- Electrocyclization of triphenylamine 19 towards carbazole 19b.

Table 2. Yields of the respective carbazole derivatives (Scheme **4B**), along with the *exo: endo* ratio, the quantum yields of reaction and the rates of cyclization expressed in μM per minute.

acetone (0.001 mol/dm 3), 50 mL 310 nm, ${\rm O}_2$, under stirring, 16 h

| | | R ⁶ T | PA R ⁵ | | R ⁶ | R5 R6 R5 | 5 | |
|-----|-----------------|------------------|---------------------------------|-----------------------|-------------------|-------------------------|------------------|-----------------------------|
| TPA | S | ubstituent | ts | carbazole | yield, and exo: | endo ratio ^b | φ _R c | rate,d |
| | R ⁴ | R ⁵ | R ⁶ | Yield, ^a % | a (exo), % | b (endo), % | | μ M min ⁻ |
| 11 | Н | CF ₃ | Н | 84 | 15 | 85 | 0.002 | 0.028 |
| 12 | Н | Н | C ₃ F ₇ | 93 | 0 | 100 | 0.001 | 0.008 |
| 13 | Н | Н | C ₄ F ₉ | 95 | 0 | 100 | 0.001 | 0.009 |
| 14 | Н | Н | C ₆ F ₁₃ | 95 | 0 | 100 | 0.001 | 0.010 |
| 15 | Н | Н | C ₈ F ₁₇ | 96 | 0 | 100 | 0.001 | 0.009 |
| 16 | Н | Н | C ₁₀ F ₂₁ | 92 | 0 | 100 | 0.001 | 0.009 |
| 17 | Н | CH ₃ | C ₄ F ₉ | 81 | 52 ^e | 48 | 0.001 | 0.006 |
| 18 | CH ₃ | CH ₃ | C ₄ F ₉ | 95 | 0 | 100 | 0.001 | 0.006 |

a.- Yield obtained by HPLC integration with internal standard. b.- relative ratio of isomers obtained through HPLC integration. c.- quantum yield obtained based on reference quantum yield of unsubstituted TPA, $\phi_I = 0.050$ in acetonitrile. ^[33] d.- rate obtained from Figure 2. e.- *Exo*-carbazole respect to methyl group

0

78

As observed form Table 2 (and Scheme 4) the yields of the sensitized photocyclization of perfluoroalkyl-substituted triphenylamines to the respective carbazole derivatives range from 78% to almost quantitative (column 5, Table 2). The high chemoselectivity towards endo cyclization of the perfluoroalkyl (R_F) substituent is striking (columns 6 and 7, Table 2). The R_F substituents are almost exclusively found in the carbazole skeleton rather substituting the 9-phenyl ancillary ring. Particularly noticeable is the case of 4-methyl-N-(4-(perfluorobutyl)phenyl)-Nphenylaniline 17 (Scheme 4, R^4 = Me, R^5 = H, R^6 = C_4F_9), with an inductively electron-donating methyl group and an inductively electron-withdrawing C₄F₉ substituents in para positions of two phenyl rings of the TPA skeleton, being the third phenyl ring unsubstituted, where upon photocyclization, the C₄F₉ substituent locates in the carbazole moiety in both the exo and endo isomers, with respect to the methyl group (vide infra products 17a and 17b, Scheme 5A). In contrast, the electron-donating methyl group is found in the carbazole entity in the endo isomer, and in the 9-

C₄F₉

C₄F₉

19

phenyl ring in the *exo* isomer, in almost an equal ratio (*exo: endo* = 52: 48) upon sensitized photocyclization. The overall yield of the electrocyclization process of **17** to yield **17a** and **17b** is 81%. Carbazoles **17a** and **17b** could not be totally separated by chromatographic techniques (column chromatography or preparative HPLC), but they were identified as separate isomers in the purified reaction mixture by a combination of spectroscopic techniques (1D and 2D NMR spectroscopy, see ESI).

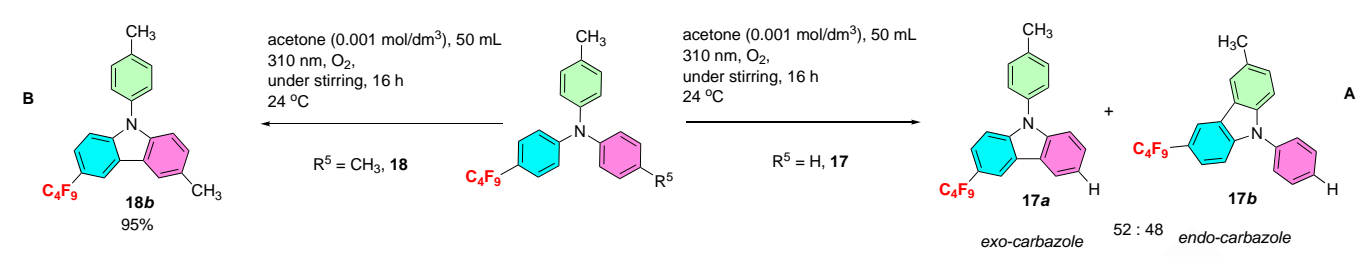
0.001

0.015

100

A more compelling example for this particular chemoselectivity and behavior of the perfluoroalkyl substituent is found in 4-methyl-N-(4-(perfluorobutyl)phenyl)-N-(p-tolyl)aniline **18** (Schemes 4B and 5B), a triphenylamine bearing two electron-donating methyl groups in para positions of two phenyl rings, and the third phenyl ring substituted with para- C_4F_9 substituent. The acetonesensitized electrocyclization process of **18** renders a single carbazole in 95% yield. A single $[6\pi]$ -electrocyclized carbazole product is observed from **18**, with the C_4F_9 substituent in the carbazole scaffold (Scheme 5B), product **18b**.

RESEARCH ARTICLE



Scheme 5. A.- Acetone-sensitized electrocyclization of 4-methyl-*N*-(4-(perfluorobutyl)phenyl)-*N*-phenylaniline 17 towards carbazoles 17a and 17b. B.- Acetone-sensitized electrocyclization of 4-methyl-*N*-(4-(perfluorobutyl)phenyl)-*N*-(p-tolyl)aniline 18 towards the exclusive formation of 3-methyl-6-(perfluorobutyl)-9-(p-tolyl

Compound **19**, 4-(perfluorobutyl)-N-(4-(perfluorobutyl))phenyl)-N-phenylaniline, with two C_4F_9 substituents in para positions of two phenyl rings of TPA, and the third phenyl ring unsubstituted, endorsed the tendency. Compound **19** underwent $[6\pi]$ -electrocyclization in acetone to carbazole **19b** (*vide supra*, Scheme 4C) in 78% yield, where the two C_4F_9 substituents are exclusively found in the carbazole unit. We investigated this marked *endo*-preference by theoretical calculations (*vide infra*). As observed from Table 2, the rates of cyclization of perfluoroalkyl-substituted TPAs **11-19** are quite low compared with other TPAs substituted with electron-donating groups **1-5** (Table 1), but nonetheless observable when compared with TPAs substituted with resonance electron-withdrawing groups (i.e.: TPAs **8-10**, Table 1), where no electrocyclization products were found, either in acetonitrile^[27a] or acetone (this study).

The progress of the photochemical reaction of amines **11–19** was monitored using chromatographic (HPLC) analyses (Figure S5, ESI). These graphs (Figure S5) are straightforward in the sense that they reveal that the disappearing of substrate (TPAs) correlates with product (carbazole) formation.

The relative yield profiles obtained from the acetone-sensitized irradiation (310 nm) of TPA (13) in an O_2 -saturated acetonitrile solution are shown in Figure S6a (ESI). The relative absorbance profiles indicate that as substrate 13 is consumed (expressed as the ratio A/A₀ at 310 nm), carbazole (13b) is formed as the only photoproduct. In Figure S6b, TPA 19 is followed as absorbance profiles indicating that as substrate 19 is consumed (expressed as the ratio A/A₀ at 310 nm), carbazole (19b) is formed as the only photoproduct.

For calculation of rate constants of cyclization (Table 2, column 9), plots of $ln(A/A_0)$ vs time are given in Figure 2, from which measurements of the observed rate constants of photosensitized irradiation of triphenylamines (11 – 19) in acetone with light of 310 nm under air atmosphere are calculated.

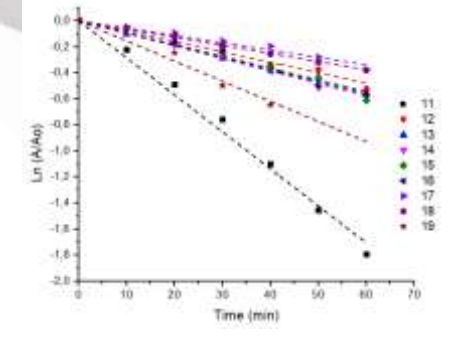


Figure 2. Measurements of the observed rate constants (k_{obs}) for irradiated triphenylamines (11-19) in acetone with light of 310 nm. Best linear regression fitting between ln(A/Ao) and time

These plots (Figure 2) indicate that TPA substituted with small CF_3 substituent (11), and TPA 19 (disubstituted with C_4F_9) are the fastest electrocyclization reactions, having the remainder perfluoroalkylated TPAs 12-18 similar cyclization rates.

The effect of substituents on the photosensitized electrocyclization reaction was also quantitatively analyzed using the Hammett linear free energy relationship through the photoreaction rate constant (*k*) according to eq 1,^[27c,d]:

$$\log(k/k_0) = \rho \sigma_p, \tag{1}$$

where k is the observed rate constant for mono-, and disubstituted triphenylamine, k_0 is the observed rate constant for unsubstituted triphenylamine, σ_p represents the Hammett substituent constants, [27c,d] and ρ is a constant reflecting the sensitivity of the photoreaction to the substituent. The observed rate constants (k) were easily determined after applying a first-order kinetic analysis for the consumption of each substituted triphenylamine in acetone solution under oxygen atmosphere ($vide\ supra$). A plot of $ln(k/k_0)$ $vs\ \sigma_p$ is illustrated in Figure 3.

A linear free energy relationship was conducted with triphenylamines **1**, **2**, **5**, **6**, **8**, **9**, **11** and **12**, whose σ_p parameters were available, and their values included in Figure 3.

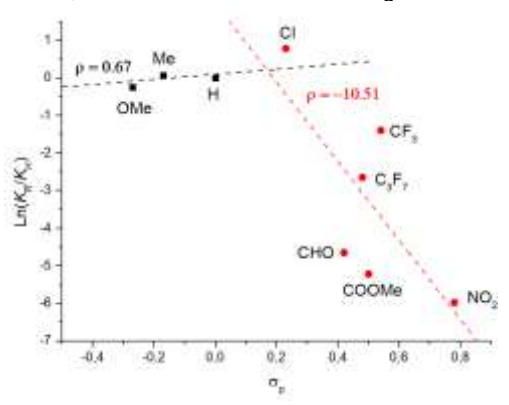


Figure 3. Hammett correlation of $ln(k_R/k_H)$ with the σ_p substituent parameters for photosensitized the irradiation of triphenylamines (1, 2, 5, 6, 8, 9, 11 and 12) in acetone with light 310 nm under air atmosphere.

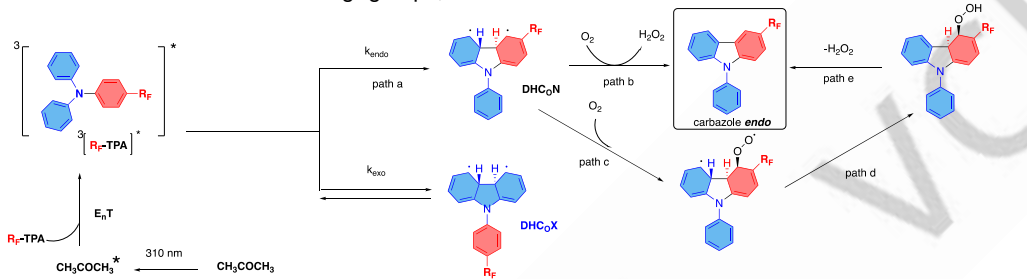
From Figure 3, it is observed that TPAs substituted with electron donating groups have a positive rho value (ρ = + 0.67), whereas TPAs substituted with electron-withdrawing groups (resonance and inductive) have a large negative rho value, (ρ = - 10.51)

RESEARCH ARTICLE

indicating a sharp deacceleration of the electrocyclization reaction with the electron poor character of the substituent. In contrast, in acetonitrile solution, [27a] the same electron donating groups show an acceleration of the electrocyclization reaction with $\rho=+$ 0.37, whereas electron-attracting groups deaccelerate the photocyclization reaction in acetonitrile, showing a $\rho=-$ 3.28. These comparative results indicate that the photocyclization of substituted TPAs is more sensitive to the substituent under photosensitization in acetone than under direct irradiation in acetonitrile solution at 254 nm.

As observed from Figure 3, the incorporation of amines **11** (CF_3) and **12** (C_3F_7) into the plot, quite adjust to the average rho value of the series of TPAs with electron withdrawing groups, as

compared with Figure S8a (ESI). The inductively electron-withdrawing perfluoroalkyl groups (such as CF $_3$, C $_3$ F $_7$, and other R $_F$ groups) slow down the photocyclization reaction compared to TPAs substituted with electron-donating groups. However, they still exhibit reactivity toward [6 π]-electrocyclization to form carbazoles, as compared with TPAs **8-10** (substituted with resonance electron withdrawing CHO, COMe, and NO $_2$ groups, respectively), whose reactivities are notably diminished by depopulation of the reactive triplet excited state due to charge transfer state formation (*vide infra*, section Photophysical Studies).[27a]



Scheme 6. Proposed reaction mechanism

A proposed reaction pathway for the photosensitized [6π]electrocyclization of R_F-TPAs by acetone is illustrated in Scheme 6. The formation of excited triplet state is definitively confirmed by sensitization in acetone. In the suggested mechanism, acetone is excited at 310 nm, resulting in the formation of excited triplet acetone following rapid and efficient intersystem crossing from the singlet excited state (E^T = 332 kJ·mol⁻¹, ϕ_{ISC} = 0.95, τ =47 μs^[31]). This triplet acetone efficiently transfers its triplet energy to R_F-TPA, assuming the triplet energy of R_F-TPA is comparable to that of TPA (295 kJ·mol -1 in MeOH) [27a], resulting in a triplet energy gap (Δ_{ET}) of -37 kJ·mol⁻¹, indicating the thermodynamic feasibility of this triplet energy transfer process. The triplet sensitized TPA undergoes electrocyclization to produce the endo diradical dihydrocarbazole intermediate DHCoN (path a, Scheme 6). DHCoN can then either react with dissolved oxygen (path b) to form endo R_F-CBz or follow path c to form a radical peroxyl intermediate, which rearranges to a hydroperoxyl intermediate (path d) that, along path e, loses H₂O₂ to yield the *endo* carbazole. An alternative exo cyclization pathway would produce intermediate DHCoX. Dihydro diradical intermediates (such as DHCoN and DHCoX) have been proposed and investigated previously using Laser Flash Photolysis.[32] It is hypothesized that the DHCoX intermediate is less favored, likely undergoing back electrocyclization, returning R_F-TPA to its ground state as the preferred deactivation pathway. Ongoing studies aim to determine the preferred [6 π]-electrocyclization pathway through a single intermediate. We performed DFT calculations to help understand this tendency (vide infra, section In Silico Studies)...

Photophysical studies

The photophysical properties of TPAs that have not previously been investigated [27,28a] are illustrated in Table 3.

For TPAs **8-10**, it was possible to carry out the UV-vis and fluorescence measurements in acetone, as the λ_{max} of absorbance are red-shifted from acetone absorption, which is not the case of TPAs **11-19**. In TPAs **8-10**, the UV-visible absorption spectra are not mirror images of the fluorescence emission spectra, indicating the presence of charge transfer states (CTS) in acetone, as was also observed in MeCN solutions. [27] The formation of these CTSs depopulate the triplet manifolds of TPAs **8-10**, responsible for [6 π]-electrocyclizations, accounting for the lack of carbazole formation. For TPAs **8-10**, the λ_{max} of the CTSs are presented in column 8, Table 3, along with the energies of the CTSs (taken from $\lambda_{(0,0)}$) in column 10, Table 3, and the quantum yields of fluorescence (column 11, Table 3).

For new TPAs 17-19, photophysical properties and parameters were studied in MeCN, MeOH, diethyl ether ad cyclohexane. The λ_{max} of absorption of 17-19 do not change significantly, being slightly red shifted with the more polar solvents (MeOH and MeCN) with respect to non-polar solvents (diethyl ether and cyclohexane). For TPAs 17 and 18, the fluorescence emission spectra are not mirror images of their absorption spectra in all the solvents studied, indicating the presence of CTSs in the excited states. Figure 4 illustrates these spectra for compounds 17 and 18 in MeCN (see ESI for spectra in other solvents). For compounds 17 and 18, the Stokes shifts (column 9, Table 3) are pronounced in polar MeCN and MeOH, and smaller in diethyl ether and cyclohexane, in agreement with CTSs being more stabilized in polar than non-polar solvents. Congruent with this observation, the λ_{max} for CTS states of 17 and 18 diminish as solvent polarity decreases.

RESEARCH ARTICLE

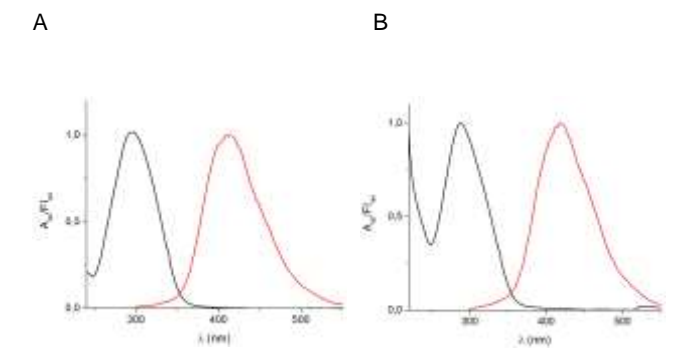


Figure 4. A.- Relative absorption (black) and emission (red) spectra of 17 in MeCN. B.- Relative absorption (black) and emission (red) spectra of 18 in MeCN

The quantum yields of fluorescence of 17-19 increase as the solvent polarity decreases, being highest in cyclohexane, where

the CTSs are less prominent, as revealed by the Stokes shifts (Stoke shifts vary from 7054 to 11042, as solvent polarity increases, column 9, Table 3) in the non-polar alkane solvent. For compound 19, no charge transfer state was encountered, being the fluorescence emission spectra mirror images of the absorption spectra in all solvents studied (section 11.3, ESI). For compound 19, λ_{max} of fluorescence decreases as solvent polarity decreases (column 4, Table 3), and the Stokes shifts vary between 5441 and 2974, as solvent polarity decreases.

For carbazoles **17b-19b**, the UV-visible spectra in acetonitrile match the fluorescence emission spectra, as revealed by the small Stokes shifts observed (column 5, Table 4). The absorption and fluorescence emission spectra of carbazoles **17b-19b** are shown in section 13, ESI. From Table 4, it can be observed that for carbazoles **17b-19b**, similar λ_{max} of absorption and emission are found in MeCN as solvent (columns 3, and 4, respectively, Table 4). The quantum yields of fluorescence for **17b-19b** in MeCN solution range between 0.07 for **17b** to 0.045 for **19b** (column 8, Table 4)

Table 3. Spectroscopic Data and Energies (ΔE) of Mono-, Di-, and Trisubstituted Triphenylamine in Acetonitrile at 298 K. Photophysical properties: λ_{max} of absorption, and fluorescence emission, Stokes shift (ΔU), wavelength of S¹ state ($\lambda_{(0,0)}$), energy of S¹ state (ΔE), Stokes shifts of charge transfer states CTS (ΔU_{CTS}), energy of CTS (ΔE_{CTS}) and quantum yield of Fluorescence (ϕf) of TPAs **17-19** in acetone, acetonitrile, methanol, diethyl ether, and cyclohexane. Photophysical data for TPAs **1-7** and **11-16** were reported elsewhere^[27,28a]

| TPA a | Solvent | λ ^m abs (nm) | λ ^m f (nm) | ΔU ^b (cm ⁻ | λ ^(0,0) (nm) | ΔΕ (0,0) (eV) | λ ^{CTS} f (nm) | ΔU ^{CTS} (cm ⁻¹) ^b | ΔE ^{CTS} (eV) | фf |
|----------|-------------------|-------------------------------|--------------------------|-------------------------------------|----------------------------|---------------------|----------------------------|---|---------------------------|-------|
| 8 | | 351 | - | -/ | 406 | 3.05 | 503 | 8609 | 2.46 | 0.153 |
| 9 | Acetone | 395 | - | - / | 427 | 2.90 | 469 | 3994 | 2.64 | 0.000 |
| 10 | | 344 | - | - | 393 | 3.15 | 473 | 7928 | 2.62 | 0.130 |
| 17 | | 294 | - | - | 352 | 3.52 | 409 | 9567 | 3.03 | 0.057 |
| 18 | MeCN | 286 | - | - | 353 | 3.51 | 418 | 11042 | 2.97 | 0.057 |
| 19 | | 319 | 386 | 5441 | 345 | 3.59 | - | - | - | 0.133 |
| 17 | | 294 | - A | - // | 349 | 3.55 | 405 | 9322 | 3.06 | 0.046 |
| 18 | MeOH | 286 | 1 | -/// | 349 | 3.55 | 412 | 10693 | 3.01 | 0.035 |
| 19 | | 318 | 373 | 4637 | 342 | 3.62 | - | - | - | 0.130 |
| 17 | | 289 | -// | //- | 346 | 3.58 | 384 | 8560 | 3.22 | 0.057 |
| 18 | Et ₂ O | 287 | - 7 | - | 348 | 3.56 | 391 | 9268 | 3.17 | 0.180 |
| 19 | | 317 | 361 | 3845 | 340 | 3.65 | - | - | - | 0.293 |
| 17 | | 289 | w - | - | 337 | 3.68 | 363 | 7054 | 3.42 | 0.133 |
| 18 | Су | 287 | - | - | 339 | 3.66 | 368 | 7669 | 3.37 | 0.146 |
| 19 | | 317 | 350 | 2974 | 336 | 3.68 | - | - | - | 0.317 |

a.- The concentration of the substrates was 5.0×10^{-5} mol·dm⁻³. b.- Calculated as follows: $\Delta v = 10^7 [1/\lambda_{abs} - 1/\lambda_{fluo}]$ cm⁻¹.

Table 4. Photophysical properties: λ_{max} of absorption (λ_{abs}^{M}), and fluorescence emission (λ_{f}^{M}), Stokes shift (ΔU), wavelength of S¹ state ($\lambda_{(0,0)}$), energy of S¹ state ($\Delta E_{(0,0)}$), and quantum yield of fluorescence (ϕ f) of carbazoles **17b-19b** in acetonitrile. Photophysical properties of carbazoles **2a-10a**, **2b-16b** were reported elsewhere. [27,28a]

| Carbazole ^a | Structure | λ ^M abs (nm) | λ ^M f (nm) | Δv ^b (cm ⁻¹) | λ ^(0,0) (nm) | ΔΕ ^(0,0) (eV) | ф |
|------------------------|-------------------------------|----------------------------|--------------------------|--|----------------------------|-----------------------------|-------|
| N-PhCBz | | 339 | 341 | 147 | 340 | 3.64 | 0.104 |
| 17 <i>b</i> | C ₄ F ₉ | 340 | 358 | 1479 | 344 | 3.60 | 0.070 |
| 18 <i>b</i> | CH ₃ | 344 | 364 | 1597 | 349 | 3.55 | 0.064 |
| 19 <i>b</i> | C_4F_9 | 332 | 346 | 1219 | 336 | 3.69 | 0.045 |

a.- The concentration of the substrates was 5.0×10^{-5} mol·dm⁻³. b.- Calculated as follows: $\Delta v = 10^{7} [1/\lambda_{abs} - 1/\lambda f_{luo}]$ cm⁻¹.

In Silico Studies

To gain a more thorough understanding of the photoinduced $[6\pi]$ electrocyclization mechanisms and the observed regioselectivity, DFT calculations were conducted on the reaction profiles associated with the transformation of the triplet state of some selected triarylamines to the corresponding N-aryl-4a,4bdihydrocarbazole (see Scheme 6) in their singlet ground state (1DHC₀). Triphenylamine 1, mono substituted triphenylamines (6, 9, 11) and a disubstituted triphenylamine (17) were selected as representative probes to carry out the computational study of the photoreaction. The free energy profiles for the $[6\pi]$ electrocyclization pathway of the triplet state of compounds 6, 11 and 17 are depicted in Figure 5. The relative free energy values $(\Delta G_{(S0-T1)})$ of triarylamines **6**, **11** and **17** are also shown in Figure 5 along with the energy values of the transition structure (TS) and the triplet (3DHC₀) and singlet (1DHC₀) substituted N-aryl-4a,4bdihydrocarbazoles which were calculated relative to the corresponding triplet state of triarylamine

Furthermore, the optimized geometries of the TSs are also included in Figure 5 displaying the C–C bond forming distances (Å). The free energy profiles for the $[6\pi]$ -electrocyclization pathway of the triplet state of triarylamines 1 and 9 have also been calculated and are collected in Figures S9 and S12, respectively (see ESI).

All the relevant data obtained from theoretical calculations in terms of $\Delta G_{(S0 \to T1)}$, relative free energies of transition states and triplet and singlet *N*-aryl-4a,4b-dihydrocarbazoles and C-C bond forming distances in the TSs are collected in Table 5. Additionally, the experimental carbazole yields are also shown in the same table for a better understanding of the theoretical and experimental correlation. Furthermore, the Mulliken spin densities of the TSs were also calculated, and these values are displayed on the corresponding isosurfaces (see Figures S14 in the ESI).

Table 5. Relative free energies for the cyclization reaction of triplet reactants (in kcal·mol⁻¹) and C–C forming bond distances in the TSs ($d_{\text{C-C}}$, in Å).

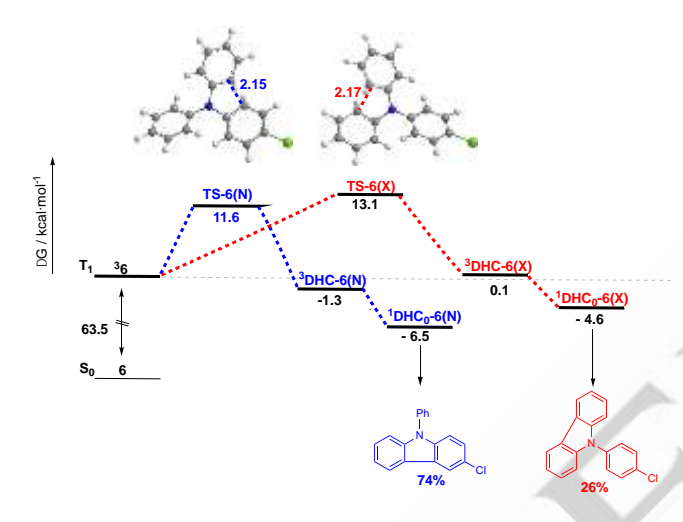
| Nº | TPA | Path | $\Delta G(S_0{\to}T_1)^a$ | TSb | ³ DHC ^b | ¹DHC₀b | $d_{	ext{C-C}}$ | Carbazole Yields (%) |
|----|------------------|------------------|---------------------------|------|-------------------------------|--------|-----------------|-------------------------|
| 1 | | | 66.6 | 9.6 | -3.4 | -8.3 | 2.17 | 100 |
| | | N° | | 11.6 | -1.3 | -6.5 | 2.15 | 74 |
| 6 | N CI | X^d | 63.5 | 13.1 | 0.1 | -4.6 | 2.17 | 26 |
| | | N° | | 13.6 | 1.0 | -4.3 | 2.14 | 85 |
| 11 | F ₃ C | X^{d} | 62.1 | 15.4 | 2.2 | -1.7 | 2.19 | 15 |
| | | N ^c | | 32.8 | 22.6 | 18.6 | 1.93 | 0 |

RESEARCH ARTICLE

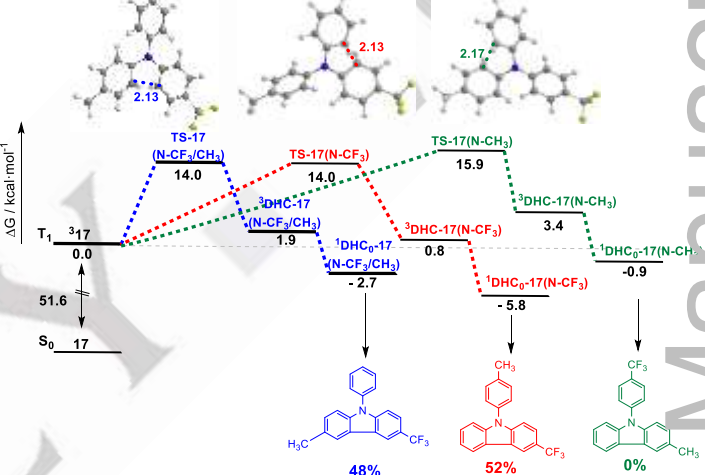
| 9 | NO ₂ | X^{d} | 39.9 | 37.3 | 24.2 | 22.2 | 2.03 | 0 |
|----|--|-------------------------------------|------|------|------|------|------|----|
| | N°-CF ₃ /CH ₃ N°-CF ₃ N°-CF ₃ N°-CH ₃ | N°-CF ₃ /CH ₃ | | 14.0 | 1.9 | -2.7 | 2.13 | 48 |
| | | | 14.0 | 0.8 | -5.8 | 2.13 | 52 | |
| 17 | | | 61.6 | | | | | |
| | C ₄ F ₉ CH ₃ | | | 15.9 | 3.4 | -0.9 | 2.17 | 0 |

a Difference in free energies between the excited triplet state and the ground state of the reactants; b.- All the energy values were computed relative to the corresponding triplet energy of the reactants; c.- N denotes the *endo* cyclization pathway; d.- X denotes the *exo* cyclization





(c) Compound 17.



(b) Compound 11.

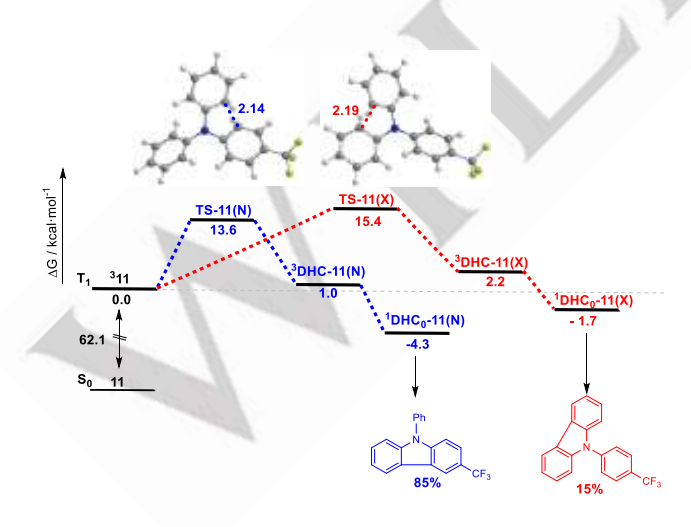


Figure 5. Free energy profiles for the cyclization of triplet states of: (a) **6** and (b) **11**, considering the two reaction pathways: endo (N) (blue) and exo (X) (red); and (c) **17** considering the three reaction pathways: N-CF₃/CH₃ (blue), N-CF₃ (red), and N-CH₃ (green). For compound **17** the CF₃ group was used as a model to represent the C₄F₉ group. All energy values are given relative to the triplet state of the reactant. The relative free energy values ($\Delta G_{(S0-T1)}$) for the reactants are also shown. Optimized geometries of the TSs are displayed, along with the C–C forming bond distances (Å).

The computational results obtained for triphenylamine (1) show that triplet state (31) leads to *trans-N*-phenyl-4a, 4b-dihydrocarbazole in the triplet state (3DHC-1) through a [6 π]-electrocyclization pathway involving the transition structure TS-1 depicted in Figure S9 (see ESI). As is apparent from the figure, the carbon atoms involved in the formation of the new C–C bond in the TS-1 are brought significantly closer ($d_{C-C} = 2.17 \text{ Å}$) to each other enabling the cyclisation process with an energy barrier of 9.6 kcal·mol⁻¹. The two unpaired triplet spins in the TS-1 are symmetrically distributed over both rings participating in the photocyclization process, as can be clearly observed from Figure S14 (see ESI). The free energy of formation for 3DHC-1 is -3.4 kcal·mol⁻¹, indicating that the electrocyclization pathway is an

WILEY ** VCH

exergonic process. Then, $^3DHC-1$ converts to the singlet ground state $^1DHC_0-1$ through an intersystem crossing pathway (ISC) which is more stable by 1.5 kcal·mol $^{-1}$. These theoretical calculations agree with those results previously obtained using the AM1-SCI method, although this latter study did not propose a transition structure. $^{[33]}$

Triplet states of monosubstituted triphenylamines **6**, **11**, and **9** (i.e.: 3 **6**, 3 **11**, and 3 **9**) can undergo [6π]-electrocyclization via two distinct cyclization pathways: *endo* and *exo* pathways, respectively. As can be seen from Figure 5, one of the two phenyl rings involved during the *endo* electrocyclic pathway bears the substituent group whereas, during the *exo* electrocyclic pathway, both phenyl rings do not bear any substituent and the substituted phenyl moiety participates to some extent in the [6π]-electrocyclic process. All the intermediates shown in Figure 5 are labelled with (N) denoting the *endo* [6π]-electrocyclization pathway and with (X) denoting the *exo* [6π]-electrocyclization pathway.

The free activation energy for the *endo* [6π]-electrocyclization pathway of triplets $^3\mathbf{6}$ and $^3\mathbf{11}$ are lower than the *exo* pathways by 1.5 and 1.8 kcal·mol⁻¹, respectively (Figures 5a,b), which could explain the selectivity of the photoreaction and the high yields of the corresponding *endo*-carbazoles. Furthermore, the formation of the triplet intermediate $^3\text{DHC-6-(N)}$ involves an exergonic process while the formation of intermediates $^3\text{DHC-6-(X)}$ and $^3\text{DHC-11-(N/X)}$ display endergonic processes. Then, these triplet intermediates deactivate efficiently through an ISC pathway yielding more stable singlet intermediates such as the corresponding $^1\text{DHC_0-6(N/X)}$ and $^1\text{DHC_0-11(N/X)}$, respectively (see Figures 5a,b).

Noteworthy, the C-C bond forming distance in TS-6-(N) and TS-11-(N) is 0.02 Å and 0.05 Å shorter, respectively, than in the corresponding exo TSs (TS-6-(X) and TS-11-(X)) indicating a more advanced [6π]-electrocyclization process in the *endo* than the exo pathways. Thus, TS-6-(N) and TS-11-(N) show higher spin densities on the phenyl ring bearing the Cl and CF₃ substituents than the unsubstituted phenyl ring displaying a notable asymmetric spin distribution (See Figure S14). This asymmetric spin distribution can be attributed to the substituents that induce a partial shift of the spin population towards their position in the phenyl ring. Conversely, the corresponding exo TSs exhibit an almost symmetric spin distribution because the substituted phenyl ring is not involved during the exo [6π]electrocyclization process as can be observed in Figures 5a,b. Therefore, this asymmetric spin distribution in the endo TSs may contribute to their stabilization.[34]

In the case of TPA 9, a TPA bearing a NO_2 group in para position of a phenyl ring, the activation barriers for TS-9(N) and TS-9(X) are significantly higher than those calculated for the other triaryl amines under study (Figure S12, ESI). Additionally, the free energies of formation of intermediates 3DHC -9(N) and 3DHC -9(X) as well as their corresponding singlet ground states, 1DHC_0 -9(N) and 1DHC_0 -9(X), confirm that these steps are highly endergonic processes. Moreover, the C–C bond forming distance values calculated for TS-9(N) and TS-9(X) are 1.93 Å and 2.03 Å, respectively (Figure S12, ESI); these shorter C-C bond distance values compared to C-C distances in TS-6,11,17 structures

reflect on a late TS that resembles to reactants, rather than products.

The spin populations in both <code>endo/exo</code> TSs (TS-9(N)) and TS-9(X)) are asymmetrically distributed over the two rings involved in C–C bond formation and onto the nitro group (Figure S14). In TS-9(N), the electron-withdrawing effect of the NO $_2$ group shifts spin density towards the phenyl ring bearing the nitro group, while in TS-9(X), most of the spin population is localized on the two phenyl rings, with a significant portion also localized on the substituted phenyl ring and on the nitro group. The spin delocalization onto the nitro group reduces the unpaired π spin density on the phenyl ring which contributes to the highest activation barriers obtained. $^{[35,36]}$

Compound **9** was found to be photochemically unreactive, and this behavior has been attributed to the formation of a charge-transfer state in the excited state between the Ph_2N- moiety and the phenyl ring bearing the NO_2 group. [37,38,27a] This spectroscopic pathway competes efficiently with the population of the photoreactive triplet state, thereby slowing or even halting the photochemical reaction. Furthermore, these calculations indicate that the $[6\pi]$ -electrocyclization of triplet 39 to form the singlet intermediates 1DHC -9(N) or 1DHC -9(X) is both kinetically and thermodynamically unfavorable under the computational calculation conditions which is consistent with the high photostability of 4-nitrophenyldiphenylamine (9). In fact, no exo/endo nitrocarbazoles were isolated after irradiation with UV light which is in line with the predictions forged from computational calculations.

The disubstituted triphenylamine 17, was also subjected to computational calculations and three possible pathways for the photocyclization reaction from triplet 3 17 have been identified (see Figure 5c). The first pathway involves both substituted rings participating in the formation of the C–C bond (pathway N-CF $_3$ /CH $_3$). In the other two pathways, only one substituted ring is involved, either the ring containing the CF $_3$ group (pathway N-CF $_3$) or the one with the CH $_3$ group (pathway N-CH $_3$) (Figure 5c). The free activation energies for TS-17(N-CF $_3$ /CH $_3$) and TS-17(N-CF $_3$) are comparable and 1.9 kcal·mol $^{-1}$ lower than that of TS-17(N-CH $_3$). This indicates that the [6 π]-electrocyclization pathways involving the phenyl ring bearing the CF $_3$ group are kinetically favored, leading to triplet intermediates that, in turn, provide the corresponding more stable singlet intermediates.

The C–C bond distances in TS-17(N-CF $_3$ /CH $_3$) and TS-17(N-CF $_3$) are comparable and shorter than those in TS-17(N-CH $_3$). The spin density distribution across the three TSs shows a similar pattern, being primarily localized on the phenyl rings involved during the cyclization process (Figure S14). In TS-17N-CF $_3$ /CH $_3$) and TS-17 (N-CF $_3$), the spin density is slightly shifted towards the ring bearing the CF $_3$ group, while in TS-17(N-CH $_3$), it is displaced towards the ring with the CH $_3$ group.

The higher activation barrier of TS-17(N-CH₃) may be attributed to the delayed formation of the C–C bond compared to the other two TSs. Furthermore, when the phenyl ring bearing the trifluoromethyl group is not directly involved in the electrocyclic reaction site, the C–C bond distances of the CF₃ substituted phenyl moiety are distorted (see Figure S14). This behavior may

RESEARCH ARTICLE

be attributed to the redistribution of electron density caused by the electron-withdrawing CF_3 group in the para position relative to the -NPh₂ moiety. [35] Similar effects are also observed in the -Ar-CF₃ and -Ar-NO₂ rings of TS-11(X) and TS-9(X), respectively. These findings suggest that the strong electron-withdrawing influence of the CF_3 and NO_2 groups, located on the non-reacting ring, may contribute to the destabilization of the associated TSs.

It is worth noting that the $[6\pi]$ -electrocyclization activation barriers for all the compounds investigated (3 6, 3 9, 3 11, and 3 17) are higher when compared to that of 3 1, consistent with experimental data indicating that substituent effects decrease the reaction rate relative to triphenylamine 1. $^{[27a]}$ Furthermore, theoretical calculation also predicted that the substituents affect the regioselectivity and the reactivity of triaryl amines during the photoinduced $[6\pi]$ -electrocyclization reaction due to changes in the electron density distributions. Therefore, the theoretical calculation results agree satisfactorily with those results obtained experimentally and rationalize the *endo* preference of TPA-R_F towards cyclization, as lower energies are obtained for both singlet and triplet dihydro diradical intermediates 3 DHC $_o$ and 1 DHC $_o$ cyclizing in *endo* manner.

Conclusion

acetone-photosensitized [6π]-electrocyclization triphenylamines bearing electron-donating groups (CH₃, OCH₃) and inductively electron-withdrawing groups (Cl, C_nF_{2n+1}) efficiently yielded carbazole derivatives in high yields, providing a practical and effective synthetic approach to the carbazole scaffold. A special case is TPA featuring an activating NH2 group in the para position of one phenyl ring, which fails to undergo electrocyclization under photosensitization in acetone due to the well-established electron transfer processes, which lead to the quenching of the ketones' triplet state by amines. Chemical yields, quantum yields of cyclization, exo/endo carbazole isomer ratios, and rates of formation were calculated for both series of TPAs in acetone solution. A comparative study in terms of Free Energy Relationship (Hammett plots) is presented in acetone and acetonitrile, showing that the reaction is more sensitive to the substituent in acetone than in previous solvents studied. Photophysical and spectroscopic data in line with absorption and fluorescence measurements are provided for both substituted triphenylamines and carbazoles, indicating that triphenylamines TPAs substituted with strong resonance electron withdrawing groups (NO2, CHO, COMe) form charge transfer states which depopulate the triplet reactive manifold. A key highlight of the study is the pronounced tendency of TPAs substituted with inductive electron-withdrawing groups (TPA-R_F/ TPA-CI) to undergo $[6\pi]$ -electrocyclization, yielding the *endo* carbazole isomer with near exclusive chemoselectivity. The propensity of TPA-R_F to form *endo* carbazole isomers was further investigated through computational studies, which show that dihydro diradical singlet and triplet intermediates DHCo formed in the endo cyclization manner are further stabilized as compared with the DHC_o exo intermediates. On going studies aim to characterize dihydrodiradical intermediates of substituted TPAs by LFP.

Supporting Information

Supporting information is provided: Synthetic procedures and general experimental considerations. UV-visible and fluorescence spectra, kinetics plots, calculation of rate constants, and copies of 1 H, 19 F, and 13 C NMR spectra are provided. Additional references are given in this section.

Acknowledgements

A.P., S.B.V., M.M.V., and S.M.B. are research members of *Consejo Nacional de Investigaciones Científicas y Técnicas*, CONICET. I.E.R. thanks CONICET for a doctoral scholarship (Doctorate Program).

We thank Centro de Cómputos de Alto Rendimiento (CeCAR) for granting the use of computational resources which allowed us to perform most of the experiments included in this work.

Keywords: EDA-complex • perfluoroalkylated triphenylamines • perfluoroalkylated carbazoles • $[6\pi]$ -electrocyclization • spectroscopy data on carbazoles •

- a) G. Wang, S. Sun, H. Guo, Eur. J. Med. Chem. 2022, 229, 113999; b)
 A. Banerjee, S. Kundu, A. Bhattacharyya, S. Sahu, M. S. Maji, Org. Chem. Front. 2021, 8, 2710–2771; c) A. Polley, K. Varalaxmi, A. Nandi, R. Jana, Asian J. Org. Chem. 2021, 10, 1207–1215; d) A. W. Schmidt, K. R. Reddy, H. J. Knölker, Chem. Rev. 2012, 112, 3193–3328; e) G. W. Gribble, Alkaloids Chem. Biol. 2012, 71, 1–165; f) W. Maneerat, T. Ritthiwigrom, S. Cheenpracha, T. Promgool, K. Yossathera, S. Deachathai, W. Phakhodee, S. Laphookhieo, J. Nat. Prod. 2012, 75, 741–746
- [2] a) D. Mousset, R. Rabot, P. Bouyssou, G. Coudert, I. Gillaizeau, Tetrahedron Lett. 2010, 51, 3987–3990; b) G. G. Rajeshwaran, A. K. Mohanakrishnan, Org. Lett. 2011, 13, 1418–1421; c) D. Crich, S. Rumthao, Tetrahedron 2004, 60, 1513–1516; d) Y. Hieda, T. Choshi, S. Kishida, H. Fujioka, S. Hibino, Tetrahedron Lett. 2010, 51, 3593–3596; e) H. J. Knölker, J. Knöll, Chem. Commun. 2003, 3, 1170–1171; f) A. Zhang, G. Lin, Bioorg. Med. Chem. Lett. 2000, 10, 1021–1023.
- [3] a) N. Senthilkumar, Y. S. Somannavar, S. B. Reddy, B. K. Sinha, G. K. A. S. S. Narayan, R. Dandala, K. Mukkanti, *Synth. Commun.* 2010, 41, 268–276; b) E. A. Dubois, J. C. Van Den Bos, T. Doornbos, P. A. P. M. Van Doremalen, G. A. Somsen, J. A. J. M. Vekemans, A. G. M. Janssen, H. D. Batink, G. J. Boer, M. Pfaffendorf, E. A. Van Royen, P. A. Van Zwieten, *J. Med. Chem.* 1996, 39, 3256–3262.
- [4] a) V. Peciuraite, S. Grigalevicius, J. Simokaitiene, J. V. Grazulevicius, J. Photochem. Photobiol. A 2006, 182, 38–42; b) S. Grigalevicius, M. H. Tsai, J. V. Grazulevicius, C. C. Wu, J. Photochem. Photobiol. A 2005, 174, 125–129; c) H. Y. Wang, F. Liu, L. H. Xie, C. Tang, B. Peng, W. Huang, W. Wei, J. Phys. Chem. C 2011, 115, 6961–6967.
- [5] a) R. M. Adhikari, D. C. Neckers, B. K. Shah, J. Org. Chem. 2009, 74, 3341–3349; b) H. Huang, Q. Fu, B. Pan, S. Zhuang, L. Wang, J. Chen, D. Ma, C. Yang, Org. Lett. 2012, 14, 4786–4789; c) X. Liu, Y. Xu, D. Jiang, J. Am. Chem. Soc. 2012, 134, 8738–8741.
- [6] a) J. Doskocz, M. Doskocz, S. Roszak, J. Soloducho, J. Leszczynski, J. Phys. Chem. A 2006, 110, 13989–13994; b) O. D. Is, F. B. Koyuncu, S.

RESEARCH ARTICLE

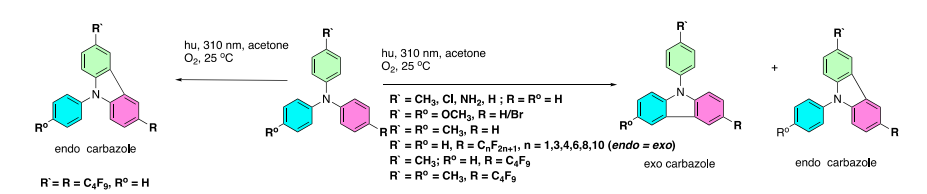
- Koyuncu, E. Ozdemir, *Polymer* **2010**, *51*, 1663–1669; c) K. S. Lee, D. U. Lee, D. C. Choo, T. W. Kim, E. D. Ryu, S. W. Kim, J. S. Lim, *J. Mater. Sci.* **2011**, *46*, 1239–1243; d) L. Wang, Y. Fu, L. Zhu, G. Cui, F. Liang, L. Guo, X. Zhang, Z. Xie, Z. Su, *Polymer* **2011**, *52*, 1748–1754.
- [7] a) T. Tsuchimoto, H. Matsubayashi, M. Kaneko, Y. Nagase, T. Miyamura,
 E. Shirakawa, J. Am. Chem. Soc. 2008, 130, 15823–15835; b) D.
 Tsvelikhovsky, S. L. Buchwald, J. Am. Chem. Soc. 2011, 133, 14228–14231; c) Q. Chen, M. Luo, Hammershøj, D. Zhou, Y. Han, B. W. Laursen,
 C. G. Yan, B. H. Han, J. Am. Chem. Soc. 2012, 134, 6084–6087.
- [8] S. Barata-Vallejo, A. Postigo, Coord. Chem. Rev. 2013, 257, 3051–3069.
- [9] a) K. Geisler, U. Koemn, Polyurethanes containing perfluoroalkyl groups and a process for their production, US 4540765 A; b) C. E. Cansoy, U. Cengiz, Colloids Surf. A: Physicochem. Eng. Asp. 2014, 441, 695–700; c) J. Xiong, L. Xia, B. Shentu, Z. Weng, J. Appl. Polym. Sci. 2014, 131, 39812-39821; d) H. Bellanger, T. Darmanin, E. Taffin De Givenchy, F. Guittard, Chem. Rev. 2014, 114, 2694–2716.
- [10] a) T. Mandal, J. Dash, Org. Biomol. Chem. 2021, 19, 9797–9808; b) J.
 Roy, A. K. Jana, D. Mal, Tetrahedron 2012, 68, 6099–6121.
- [11] I. E. Romero, A. Postigo, S. M. Bonesi, Chem. Eur. J. 2024, 30, e202303229.
- a) H. J. Knölker, K. R. Reddy, Chem. Rev. 2002, 102, 4303–4427; b) A.
 Caruso, D. Iacopetta, F. Puoci, A. R. Cappello, C. Saturnino, M. S.
 Sinicropi, Mini Rev. Med. Chem. 2016, 16, 630–643.
- [13] a) A. Caruso, A. S. Voisin-Chiret, J. C. Lancelot, M. S. Sinicropi, A. Garofalo, S. Rault, *Heterocycles* 2007, 71, 2203–2210; b) A. Caruso, A. S. Voisin-Chiret, J. C. Lancelot, M. S. Sinicropi, A. Garofalo, S. Rault, *Molecules* 2008, 13, 1312–1320; c) C. Saturnino, F. Grande, S. Aquaro, A. Caruso, D. Iacopetta, M. G. Bonomo, P. Longo, D. Schols, M. S. Sinicropi, *Molecules* 2018, 23, 286-294.
- [14] a) W. C. P. Tsang, N. Zheng, S. L. Buchwald, J. Am. Chem. Soc. 2005, 127, 14560–14561; b) J. A. Jordan-Hore, C. C. C. Johansson, M. Gulias, E. M. Beck, M. J. Gaunt, J. Am. Chem. Soc. 2008, 130, 16184–16186; c) S. H. Cho, J. Yoon, S. Chang, J. Am. Chem. Soc. 2011, 133, 5996–6005; d) B. J. Stokes, B. Jovanović, H. Dong, K. J. Richert, R. D. Riell, T. G. Driver, J. Org. Chem. 2009, 74, 3225–3228; e) B. J. Stokes, K. J. Richert, T. G. Driver, J. Org. Chem. 2009, 74, 6442–6451; f) D. S. Surry, S. L. Buchwald, J. Am. Chem. Soc. 2007, 129, 10354–10355.
- [15] For palladium, see: a) B. Liégault, D. Lee, M. P. Huestis, D. R. Stuart, K. Fagnou, J. Org. Chem. 2008, 73, 5022–5028; b) M. Yamamoto, S. Matsubara, Chem. Lett. 2007, 36, 172–173.
- [16] a) G. J. Zha, W. Ji, Z. H. Qi, W. J. Qiu, A. M. Li, D. R. Zhu, S. Jing, J. Catal. 2022, 405, 313–321; b) X. Liu, H. Sheng, Y. Zhou, Q. Song, Chem. Commun. 2020, 56, 1665–1668; c) Y. Huang, M. J. Ajitha, K. W. Huang, Z. Zhang, Z. Weng, Dalton Trans. 2016, 45, 8468–8474; d) H. Liu, J. Wu, Y. Jin, X. Leng, Q. Shen, J. Am. Chem. Soc. 2021, 143, 14367–14378.
- [17] B. Lantaño, S. Barata-Vallejo, M. R. Torviso, S. M. Bonesi, J. E. Argüello, A. Postigo, J. Fluor. Chem. 2014, 161, 149–155.
- [18] B. Chang, H. Shao, P. Yan, W. Qiu, Z. Weng, R. Yuan, ACS Sustain. Chem. Eng. 2017, 5, 334–341.
- [19] a) C. K. Prier, D. A. Rankic, D. W. C. MacMillan, Chem. Rev. 2013, 113, 5322–5363; b) S. Parisien-Collette, S. K. Collins, ChemPhotoChem 2018, 2, 855–859; c) S. Parisien-Collette, C. Cruché, X. Abel-Snape, S. K. Collins, Green Chem. 2017, 19, 4798–4803; d) A. C. Hernandez-Perez, A. Caron, S. K. Collins, Chem. Eur. J. 2015, 21, 16673–16678; e) S. Parisien-Collette, A. C. Hernandez-Perez, S. K. Collins, Org. Lett. 2016, 18, 4994–4997; f) A. C. Hernandez-Perez, S. K. Collins, Angew. Chem. Int. Ed. 2013, 52, 12696–12700.

- [20] S. Choi, T. Chatterjee, W. J. Choi, Y. You, E. J. Cho, ACS Catal. 2015, 5,4706,4902
- [21] a) Z. Qu, P. Wang, X. Chen, G. J. Deng, H. Huang, *Chinese Chem. Lett.*2021, 32, 2582–2586; b) Z. Qu, X. Ji, S. Tang, G. J. Deng, H. Huang,
 Org. Lett. 2022, 24, 7173–7177.
- [22] a) E. J. Bowen, J. H. D. Eland, *Proc. Chem. Soc. London* 1963, 202; b)
 K. H. Grellmann, G. M. Sherman, H. Linschitz, *J. Am. Chem. Soc.* 1963, 85, 1881–1882.
- [23] For irradiation of diphenylamine, see: a) H. Shizuka, Y. Takayama, I. Tanaka, T. Morita, J. Am. Chem. Soc. 1970, 92, 7270–7277; b) R. Rahn, J. Schroeder, J. Troe, K. H. Grellmann, J. Phys. Chem. 2009, 93, 7841–7846; c) H. Linschitz, K. H. Grellmann, J. Am. Chem. Soc. 1964, 86, 303–304; d) T. Suzuki, Y. Kajii, K. Shibuya, K. Obi, Bull. Chem. Soc. Jpn. 1992, 65, 1084–1088.
- [24] For irradiation of N-methyldiphenylamine, see: a) H. Shizuka, Y. Takayama, T. Morita, S. Matsumoto, I. Tanaka, J. Am. Chem. Soc. 1971, 93, 5987–5992; b) E. W. Förster, K. H. Grellmann, H. Linschitz, J. Am. Chem. Soc. 1973, 95, 3108–3115; c) G. Fischer, E. Fischer, K. H. Grellmann, A. Temizer, H. Linschitz, J. Am. Chem. Soc. 1974, 96, 6267–6269; d) K. H. Grellmann, W. Kiihnle, H. Weller, T. Wolff, J. Am. Chem. Soc. 1981, 103, 6889–6893.
- [25] For irradiation of triphenylamine, see: a) E. W. Forster, K. H. Grellman, *Chem. Phys. Lett.* 1972, 14, 536–538; b) H. Görner, *J. Phys. Chem. A* 2008, 112, 1245–1250; c) S. M. Bonesi, D. Dondi, S. Protti, M. Fagnoni, A. Albini, *Tetrahedron Lett.* 2014, 55, 2932–2935.
- [26] a) S. M. Bonesi, S. Protti, A. Albini, J. Org. Chem. 2018, 83, 8104–8113;
 b) S. M. Bonesi, M. Mella, D. Merli, S. Protti, Photochem. Photobiol. 2021,
 97, 1278–1288; c) S. Protti, M. Mella, S. M. Bonesi, New J. Chem. 2021,
 45, 16581–16593; d) R. A. Sanmartín, M. L. Salum, S. Protti, M. Mella,
 S. M. Bonesi, ChemPhotoChem 2022, 6, e202100247; e) M. L. Salum,
 S. Protti, M. Mella, S. M. Bonesi, ChemPhotoChem 2024, 8, e202400051.
- [27] a) I. E. Romero, B. Lantaño, A. Postigo, S. M. Bonesi, J. Org. Chem.
 2022, 87, 13439–13454; b) I. E. Romero, A. Postigo, S. M. Bonesi, J. Org. Chem. 2023, 88, 4405–4421; c) L. P. Hammett, Chem. Rev. 1935, 17, 125–136; d) D. F. Ewing. In Correlation of NMR chemical shifts with Hammett σ values and analogous parameters. Correlation Analysis in Chemistry: Recent Advances; Chapman, N. B., Shorter, J., Eds.; Plenum Press: New York, 1978; pp 357–396.; e) R. W. Yip, R. O. Loutfy, Y. L. Chow, L. K. Magdzinski, Can. J. Chem. 2011, 50, 3426–3431.
- [28] a) I. E. Romero, S. Barata-Vallejo, S. M. Bonesi, A. Postigo, Chem. Eur. J. 2024, 30, e202400905; b) I. Fleming. In Pericyclic reactions; Oxford University Press, 1998; c) A. Rauk. In Orbital Interaction theory of organic chemistry, Second ed.; John Wiley & Sons, Inc., 2001; Chapter 12, pp 161–174.
- [29] Y. J. Wang, X. L. Liu, Z. Z. Huang, J. W. Jiang, S. R. Sheng, J. Macromol. Sci., Part A: Pure and Applied Chemistry 2017, 54, 534–542.
- [30] a) D. E. Yerien, S. Barata-Vallejo, D. Mansilla, A. Postigo, *Photochem. Photobiol. Sci.* 2022, 21, 803–812; b) E. Mora Flores, M. L. Uhrig, A. Postigo, *Org. Biomol. Chem.* 2020, 18, 8724-8734; c) D. E. Yerien, M. V. Cooke, M. C. García Vior, S. Barata-Vallejo, A. Postigo, *Org. Biomol. Chem.* 2019, 17, 3741–3746; d) B. Lantaño, S. Barata-Vallejo, A. Postigo, *Org. Biomol. Chem.* 2018, 16, 6718–6727; e) D. E. Yerien, A. Postigo, M. Baroncini, S. Barata-Vallejo, *Green Chem.* 2021, 23, 8147–8153; f) B. Lantaño, D. E. Yerien, S. Barata-Vallejo, A. Postigo, *Photochem. Photobiol. Sci.* 2021, 20, 971–983; g) S. Barata-Vallejo, M. V. Cooke, A. Postigo, *ACS Catal.* 2018, 8, 7287–7307.

- [31] a) F. Strieth-Kalthoff, F. Glorius, Chem. 2020, 6, 1888–1903; b) S. M. Bonesi, R. Erra-Balsells, J Lumin 2001, 93, 51–74.
- [32] R. A. Sanmartín, M. L. Salumn, S. Protti, M. Mariella, S. M. Bonesi, ChemPhotoChem 2022, e202100247.
- [33] N. Chattopadhyay, C. Serpa, P. Purkayastha, L. G. Arnaut, S. J. Formosinho, *Phys. Chem. Chem. Phys.* 2001, 3, 70–73.
- [34] P. Ravat, P. Ribar, M. Rickhaus, D. Häussinger, M. Neuburger, M. Juríček, J. Org. Chem. 2016, 81, 12303–12317.
- [35] M. Baranac-Stojanović, J. Org. Chem. 2020, 85, 4289–4297.
- [36] C. Nitu, S. Crespi, J. Phys. Org. Chem. 2023, 36, e4437.
- [37] X. Zhang, C. J. Wang, L. H. Liu, Y. B. Jiang, J. Phys. Chem. B 2002, 106, 12432–12440.
- [38] V. Lucena, M. I. Quindt, S. Crespi, S. M. Bonesi, *Photochem. Photobiol. Sci.* 2022, 21, 739–753.

RESEARCH ARTICLE

Entry for the Table of Contents



The acetone-photosensitized irradiation of mono- and di-substituted triarylamines effectively affords the respective carbazoles in high yields. Particularly noticeable are triarylamines substituted with inductive electron withdrawing groups (CI, C_nF_{2n+1}), which afford almost exclusively *endo* carbazoles. Mechanistic investigations and in-silico studies rationalize this tendency.

X.com/FFYB_UBA

